Burning Velocities of CH_4/air/water-mist Premixed Flames near the Extinction Limit

Yasuhiro Ogami, Masahiro Ito, Tadafumi Daitoku and Takashi Tsuruda
Faculty of Systems Science and Technology, Akita Prefectural University
Yurihonjyo, Akita, Japan

1 Introduction

In recent years, fire suppression by water mist has been intensively investigated because of its effectiveness as fire extinguishing agent alternative to Halon gases. With respect to premixed flames, Blouquin and Jouline made theoretical study on flame inhibition by mono-disperse water mist to investigate the effect of the droplet diameter on the burning velocity [1]. Kee et al. [2] conducted numerical simulations considering a detailed chemical reaction, and the same trend as that by Blouquin and Jouline [2] was obtained. Fuss et al. [3] measured the burning velocities of stoichiometric CH_4/air/water mist premixed flames. These studies mainly focused on the effect of the droplet diameter on fire suppression, and the effect of the equivalence ratio was not sufficiently discussed. Moreover, both of experimental and numerical data near the extinction limit are still limited. In this study, measurements of CH_4/air/water-mist premixed flames were conducted in the conditions close to the extinction limit. Experiments were conducted for the two-dimensional Bunsen flames in the range of the equivalence ratio of 0.8-1.3. Estimation of heat losses due to water mist was conducted, and the correlation between the burning velocity and the heat loss parameter was investigated.

2 Experimental Method

Figure 1 shows a schematic of the experimental setup. The experimental apparatus employed in this study consists of the water supply system, the water-mist generator, the extension tube, and the slot-type nozzle burner. Distilled water was continuously supplied to the water-mist generator so that the water level was constant. Atomization of water was done by the ultrasonic transducer which was placed on the bottom of the water-mist generator. Air and CH_4 whose flow rates were controlled by mass flow controllers were also supplied from upper part of the water-mist generator, and the gas-liquid two-phase flow was introduced to the extension tube. Two types of the extension tube with a different cross-sectional area, A, were employed, that is, A, for the case-1 was twice as that of the case-2. This makes it possible to vary the mass fraction of water mist, as mentioned later. The gas-liquid two-phase flow was supplied to the slot-type nozzle burner whose exit size and nozzle contraction ratio were 8 mm × 30 mm and 10, respectively. Two premixed pilot flames were formed on both sides of the main premixed flame to strengthen the flame base, as the ability to hold the flame was very low in the water-mist added conditions. The amount of methane/air mixture supplied for the pilot flames was less than 5 % of that for the main premixed flame. The burner exit was enclosed by a

Correspondence to: ogami@akita-pu.ac.jp

cubic cover made of quartz glass to separate the hot combustion gas and the cold surrounding gas. This made it possible to limit the effects of the disturbances and buoyancy due to the surrounding cold gas. Additionally, it is possible to exclude the influence on the flammability of the inner premixed flame due to the outer flame (i.e., the diffusion flame) even in the fuel-rich conditions, because the Smithells flame is formed by using the glass cover which prevents supply of oxygen to excess fuel. All devices were placed on the electronic balance, and the mass flow rate of water can be measured during experiments.

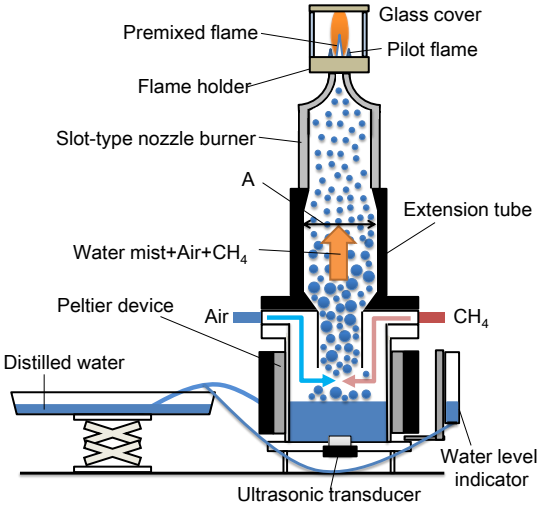

Figure 1. Schematic of experimental apparatus.

3 Estimation of Water Mist Characteristics

Prior to the combustion experiment, the relationship between the burner-exit gas velocity, U_{exit} [m/s], and the water mass flow rate, $\dot{M}_{water}$ [kg/s] was measured. By subtracting the mass flow rate of the saturated vapor, $\dot{M}_{saturate}$ [kg/s], from $\dot{M}_{water}$, the water-mist mass flow rate, $\dot{M}_{mist}$ [kg/s], can be derived. $\dot{M}_{saturate}$ was evaluated by assuming saturation at 293 K.

The maximum droplet size, D_{max} [m], can be obtained by Stokes' law:

$$D_{max} = \sqrt{18\mu_g U_g / (\rho_{H2O} - \rho_g) g}\,,$$

where U_g [m/s] is the gas velocity inside the burner (i.e, 1/10 of U_{exit}), ρ_{H2O} [kg/m^3] is the water density, ρ_g [kg/m^3] is the gas density, g [m/s^2] is the acceleration of gravity, and μ_g [Pa · s] is the gas viscosity. $\dot{M}_{mist}$ [kg/s] can be expressed as follow:

$$\dot{M}_{mist} = \int_0^{M_{D_{max}}} \dot{N}\, dM_D,$$

where $M_{D_{max}}$ [kg] is the mass of droplet with the diameter of D_{max}, $\dot{N}$ [1/s] is the droplet number density per unit time. By differentiating both sides of the above equation with $M_{D_{max}}$, $\dot{N}$ can be derived.

Figure 2 shows the droplet size distribution of the water mist for the case-1 and the case-2. Because the same ultrasonic transducer was used, only small difference can be seen between two cases. As shown in Stokes' law, D_{max} depends on U_g ($\propto U_{exit}$). Accordingly, it can be assumed that only droplets with smaller diameter than D_{max} are contained at the burner exit when U_{exit} is fixed at a certain value. In this study, the droplet size distribution was controlled by varying U_{exit}.

Figure 3 shows the variation the water-mist mass fractions, Y_{mist}, the saturated-vapor mass fraction, $Y_{saturate}$, and the volume length average particle diameter, D_{31} [m]. $Y_{suturate}$ are generally constant

in both cases. Y_{mist} increases with decreasing U_{exit} in the rage of U_{exit} of 0.4 to 1.0 m/s in both cases. The value of Y_{mist} in the case-2 is about twice as that for the case-1. D_{31} decrease with the decrease of U_{exit} in the range of U_{exit} of 0.4 to 1.0 m/s in both cases.

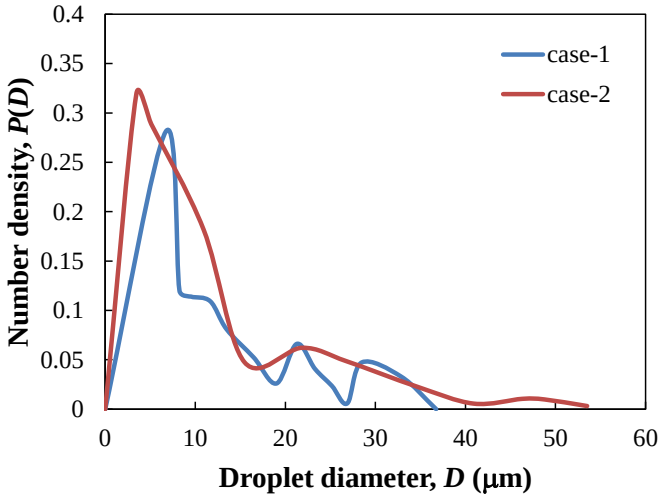

Figure 2. Droplet size distribution.

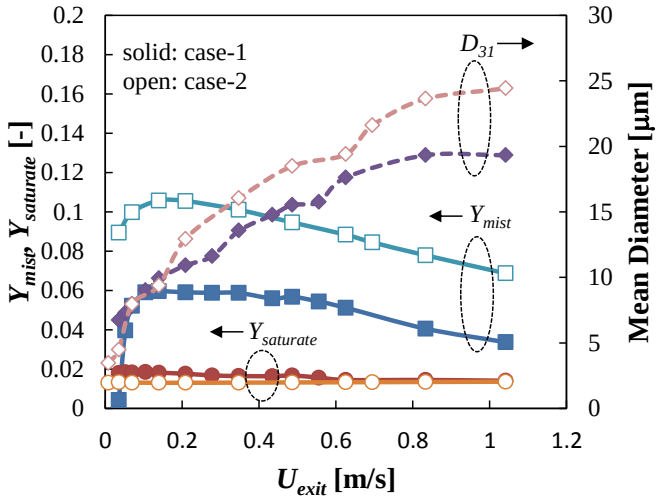

Figure 3. Mass fractions and mean diameter.

4 Extinction limit of CH_4/air/water-mist premixed flame

Combustion experiments were conducted in the ranges of the equivalence ratio, ϕ, of 0.8 to 1.3 and U_{exit} of 0.4 to 1.0 m/s for the case-1 and the case-2.

Figure 4(a) and (b) show direct images of the CH_4/air/water-mist premixed flame (ϕ = 1.1) for the case-2 in the conditions with U_{exit} = 1.0 and 0.6 m/s, respectively. In the case of $U_{exit} = 1.0\ m/s$ (Fig. 4(a)), a stable triangle-shaped flame is formed, and intense radiation is emitted from evaporated vapor in the burnt gas region. When U_{exit} is decreased to 0.6 m/s (Fig. 4(b)), radiation from vapor becomes weaker, and the flame is no longer able to maintain a triangular shape. This is because the flame is weakened by the increase of Y_{mist} and the decrease of D_{31} accompanying the decrease in U_{exit}. Although the flame is barely maintained by the pilot flames, such the flame cannot be regarded

as a premixed flame and considered as a kind of a diffusion flame. In this study, the extinction limit was determined as a condition in which the flame shape changes largely when U_{exit} is reduced as shown in Fig. 4.

Figure 5 shows the variation of the mass fraction of added water, Y_{water} ($= Y_{mist} + Y_{saturate}$), at the extinction limit. The result shows that Y_{water} has a peak around ϕ = 1.2, indicating that flame extinction is less likely to occur in the fuel-rich conditions.

Sasongko et al. [4] have proposed that the vaporization Damkőler number, Da, can be obtained by the following equation:

$$Da = \frac{K\alpha}{D_{31}^2 S_u^2},$$

where $K\left[\mathrm{m}^2/\mathrm{s}\right]$ $(= 1 \times 10^{-6})$ is the vaporization rate constant of water, S_u [m/s] is the burning velocity, α [m^2/s] is the thermal diffusivity. If Da is less than unity, the mass fraction of evaporated water in the flame zone, Y_{vapor}, can be evaluated by the following equation:

$$Y_{vapor} = \frac{3}{2} Y_{mist} Da.$$

S_u were determined by the angle method, and Da were estimated; however they were small enough and $Da \gg 1$ can be attained in the all conditions, indicating that water mist was completly evaporated in the flame zone. This is consistent with the flame observation shown in Fig. 4(a) which is in the severest condition for evaporation, that is, the black zone without water mist can be seen just befor the blue flame. Accordingly, Y_{vapor} is identical to Y_{mist} in the all conditions in this study.

There are four types of the heat loss due to water mist, i.e., the latent heat of vaporization of water mist, L_{latent}, the sensible heat of vapor generated from water mist, L_{vapor}, the sensible heat of saturated vapor, $L_{saturate}$, and the sensible heat of liquid water, L_{liquid}. If the flame temperature is evaluated, all of above heat losss can be estimated. In this study, the flame temperature was determined by the chemical equilibrium calculation software NASA-CEA [5] using data of Y_{vapor}. In addition, the radiative heat losses from vapor and combustion gas are expected: however, they are much smaller than above-mentioned heat losses [1]. Therfore, the radiative heat losses are not considered in this study.

Estimated values of the heat losses at the extinction limit are also shown in Fig. 5. All heat loss data are normarized by the heat of reaction. The total heat loss, L_{total} (i.e., the heat loss parameter), has a peak at ϕ = 1.2. In all conditions, L_{vapor} is the largest and account for a half of L_{total}.

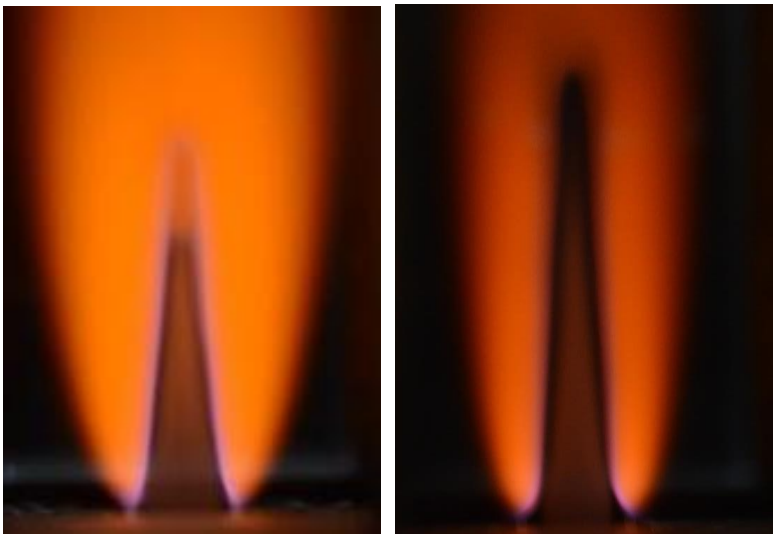

(a) $U_{exit} = 1.0$ m/s (b) $U_{exit} = 0.6$ m/s

Figure 4. Direct image of CH_4/air/water-mist premixed flame (case-2, ϕ = 1.1).

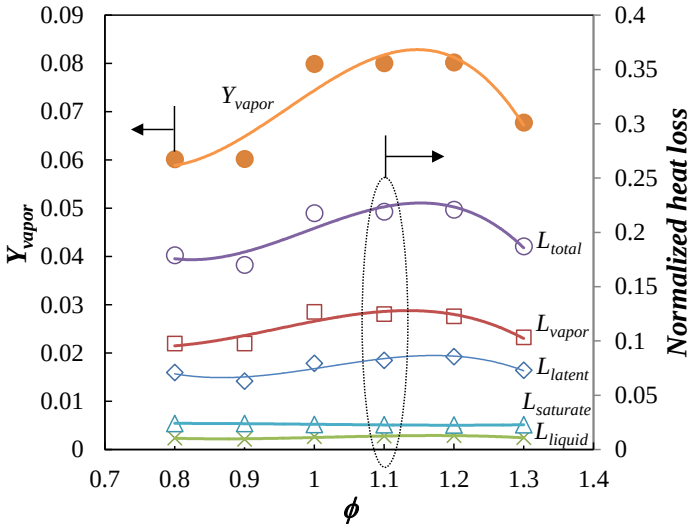

Figure 5. Extinction limit and heat losses.

5 Burning velocity of CH4/air/water-mist premixed flame

Figure 6 shows the relationship between the normalized burning velocity, $S_u/S_u{}^0$ ($S_u{}^0$: the burning velocity without water mist), and Y_{vapor}. $S_u{}^0$ were obtained experimentally for the flame with wet air as the oxidizer. In Fig. 5, the extinction limits are also shown. Experimental data can be classified into 2 groups, i.e., the group-1 with higher buring velocities (ϕ = 0.9, 1.0, and 1.1) and the group-2 with lower burning velocities (ϕ = 0.8, 1.2, and 1.3). These groups correspond to the difference in the flame temperature, that is, the flame temperature of the group-1 is higher than that of the group-2. Within each group, the value of L_{total} at the extinction limit becomes larger as ϕ increases. These results indicate that the flame suppression effect is more significant in the group-2 for the same heat loss parameter, although the extinction limit seems to strongly depend on the equivalence ratio rather than the flame temperature.

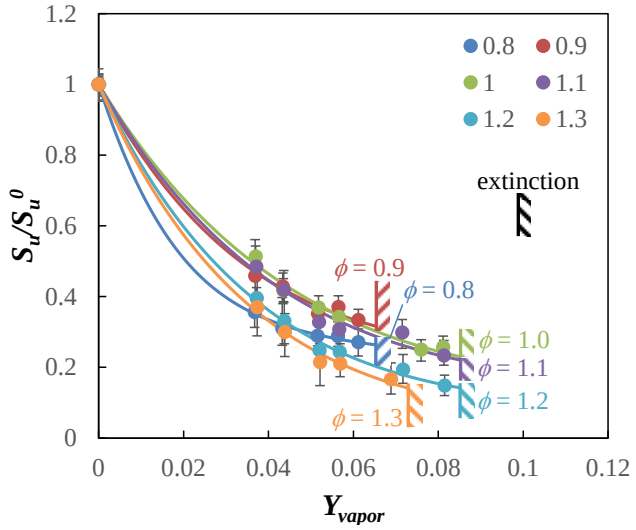

Figure 6. Variation of normalized burning velocity to Y_{vapor}.

6 Conclusions

Combustion experiments of CH_4/air/water-mist premixed flames were conducted using the two-dimensional Bunsen flames. The extinction limit was determined for the conditions of the equivalence ratios of 0.8 to 1.3. It was found that the mass fraction of added water at the extinction limit has a peak at the equivalence ratio of 1.1, indicating that flame extinction is less likely to occur in the fuel-rich conditions. The burning velocities of CH_4/air/water-mist premixed flames were also measured. Results show that the flame surpression effect is more significant in the conditions with the lower flame temperature (i.e., ϕ = 0.8, 1.2, and 1.3) for the same heat loss parameter despite the strong dependence of the extinction limit on the equivalence ratio.

References

[1] Blouquin, R., Joulin, G. (1998). On the quenching of premixed flames by water sprays: influences of radiation and polydispersity. Proc. 27th Symp. (int.) Combst.: 2829-2837.

[2] Yang, W., Kee, R.J. (2002). The effect of monodispersed water mists on the structure, Burning velocity, and extinction behavior of freely propagating, stoichiometric, premixed, methane-air flames. Combust. Flame 130: 332-335.

[3] Fuss, S.P., et al. (2002). Inhibition of premixed mehane/air flames by water mist. Proc. Combust. Inst. 29: 361-368.

[4] Sasongko, et al. (2011). Extinction condition of counterflow diffusion flame with polydisperse water sprays. Proc. Combust. Inst. 33: 2555-2562.

[5] Gordon, S., and McBride, B.J. (1996). NASA Reference Publication 1311.